PHYSICAL REVIEW B **82**, 085410 (2010)

Spin detection at elevated temperatures using a driven double quantum dot

G. Giavaras,[1] J. Wabnig,[1,2] B. W. Lovett,[1] J. H. Jefferson,[3] and G. A. D. Briggs[1]
[1]*Department of Materials, University of Oxford, Oxford OX1 3PH, United Kingdom*
[2]*Cavendish Laboratory, Department of Physics, University of Cambridge, Cambridge CB3 0HE, United Kingdom*
[3]*QinetiQ, St. Andrews Road, Malvern WR14 3PS, United Kingdom*
(Received 8 December 2009; revised manuscript received 9 June 2010; published 6 August 2010)

We consider a double quantum dot in the Pauli blockade regime interacting with a nearby single spin. We show that under microwave irradiation the average electron occupations of the dots exhibit resonances that are sensitive to the state of the nearby spin. The system thus acts as a spin meter for the nearby spin. We investigate the conditions for a nondemolition read-out of the spin and find that the meter works at temperatures comparable to the dot charging energy and sensitivity is mainly limited by the intradot spin relaxation.

DOI: 10.1103/PhysRevB.82.085410 PACS number(s): 85.35.−p, 73.63.Kv, 73.23.Hk

I. INTRODUCTION

Electron spins in semiconductors and molecular systems are good candidates for qubits due to their relatively long coherence times. Manipulation of single spins and controlled interaction between pairs of spins are essential ingredients for quantum information processing. Single spin rotation has been demonstrated in electrostatically defined quantum dots using the electron-spin-resonance technique.[1] Coherent manipulation of a pair of qubits, giving rise to entanglement, has also been achieved in a semiconductor double dot (DD) device based on fast electrical pulses and operating the dots in the spin blockade regime.[2] Single spin rotations together with entanglement generation, in principle, enable universal quantum operations. A further operation for a quantum processor is spin detection, which is essential for projection of the quantum state after computation and read-out of the result. This is the main focus of this paper.

Single spin detection is also important for future spintronic devices in general, and various electrical and optical schemes have been proposed and demonstrated. For example, Elzerman *et al.*[3] demonstrated experimentally a single-shot read-out of a quantum dot spin using a spin to charge conversion technique while Rugar *et al.*[4] employed magnetic resonance force microscopy to probe the state of a single spin. Theoretically, spin filters and spin pumps which make use of excited states in ac-driven DDs have been examined.[5,6] Other schemes for spin read-out involve open quantum dots with an inhomogeneous Zeeman splitting and closed DD systems which are coupled to quantum point contacts (QPCs).[7,8] It has been shown that the dc-electrical current and shot noise through the dots or the point contacts can provide valuable information about the spin state, the energy spectrum, and the relevant decoherence rates.[7,8] However, for optically nonactive molecular spins no reliable read-out scheme exists.

In this work we consider a single spin (target spin) that interacts with the spins of two tunnel-coupled quantum dots, as shown schematically in Fig. 1, and demonstrate how to probe its state by monitoring the average electron occupation on one of the two dots. Under a range of parameters, the interaction between the target spin and the spins on the DD induces an effective Zeeman splitting that is different in each dot. Also, the sign of the Zeeman splitting depends on the orientation of the target spin. This target-spin-dependent asymmetry of the Zeeman splitting makes it possible to rotate only one of dot spins and thus results in a target-spin-dependent lifting of the Pauli blockade. We show this lifting of the blockade as a change in the average dot occupation, which can be measured by a charge detector. Alternatively, the change in occupation is directly related to a change in the current through the DD, which, however, might be too small to detect by standard dc-measurement techniques.

In order to realize a nondemolition spin measurement the spins on the DD and the target spin must have different Zeeman splitting, most likely to be achieved by different g factors through g-factor engineering or choice of materials. A general spin-spin interaction always contains so-called spin-

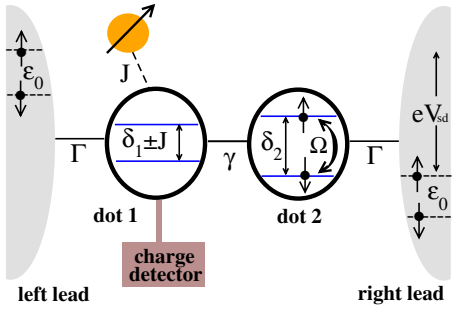

FIG. 1. (Color online) Schematic illustration of the proposed system for a single spin detection. Two tunnel-coupled quantum dots are connected to leads enabling current to pass through. A nearby spin interacts with the spins on dot 1 and under a range of parameters, this interaction induces a different Zeeman splitting in the two dots. In an external magnetic field and under microwave irradiation the spins on the two dots can be rotated with a Rabi frequency Ω and the average electron occupation exhibits resonances which are sensitive to the state of the nearby spin. A charge detector is capacitively coupled to dot 1 and is used to monitor a change in the occupation. In the rotating frame with respect to the incident microwave field the lead electrons have a Fermi energy that depends on their spin state with a relative energy difference $\varepsilon_0=\hbar\omega_0$, where ω_0 is the frequency of the driving magnetic field. V_{sd} is the bias voltage across the dots. The effective Zeeman splitting in each dot, $\delta_1 \pm J$ and δ_2, respectively, depends on both the orientation of the nearby spin and the interaction strength J.

flip terms, which are suppressed when the difference in the Zeeman splitting of the DD electrons and the target spin is larger than the spin-spin interaction strength.

A theoretical investigation has shown that a single quantum dot works as a spin meter, but the proposed device has the drawback of operating only at low temperatures, comparable to the energy scale set by the Zeeman spitting.[9] In this paper we show that the driven DD spin detector works at much higher temperatures, comparable to the DD charging energy and we find that the main limitation to its sensitivity is intradot spin relaxation. Thus we present a scheme that allows the spin state of a nearby spin to be probed noninvasively in a single shot, using different electron occupations on the DD for spin up and spin down orientations as a basic read-out mechanism.

In the following section we introduce our model and discuss technical details of the solution. In Sec. III we show how the DD acts as a spin meter and explore how interdot hopping, microwave intensity, temperature, spin-spin interaction strength, and spin relaxation influence its performance. We conclude in Sec. IV by discussing the operation of the spin meter for experimentally accessible parameters.

II. PHYSICAL MODEL

The total system consists of the DD, a nearby spin, metallic leads, and a bosonic heat bath. This system is modeled by the Hamiltonian

$$H_{tot} = H_S + H_{leads} + H_T + H_B + H_{SB}, \tag{1}$$

where H_S models the DD and the spin, H_{leads} (H_B) models the leads (heat bath), and H_T (H_{SB}) models the interaction between the leads (heat bath) and the DD. Specifically, for the DD and the nearby target spin we write the Hamiltonian as

$$H_S = H_{\mathrm{DD}} + H_M + H_I, \tag{2}$$

where H_{DD} is a Hubbard Hamiltonian describing the DD, H_M is due to the applied magnetic fields, and H_I models the interaction of the nearby spin with the DD system. For the DD we have

$$H_{\mathrm{DD}} = \sum_{i=1}^{2} \varepsilon_i n_i - \gamma \sum_{\sigma} (c_{1\sigma}^{\dagger} c_{2\sigma} + c_{2\sigma}^{\dagger} c_{1\sigma}) + U \sum_{i=1}^{2} n_{i\uparrow} n_{i\downarrow} + V n_1 n_2, \tag{3}$$

that allows up to two electrons per dot.[10] The number operator is $n_i = \Sigma_\sigma n_{i\sigma} = \Sigma_\sigma c_{i\sigma}^{\dagger} c_{i\sigma}$ for dot $i = \{1,2\}$ and spin $\sigma = \{\uparrow, \downarrow\}$. The operator $c_{i\sigma}^{\dagger}$ ($c_{i\sigma}$) creates (annihilates) an electron on dot i with on-site energy ε_i. γ is the tunnel coupling between the two dots, U is the charging energy (intradot Coulomb energy), and V is the interdot Coulomb energy. The Hamiltonian part due to the applied magnetic fields, that breaks the spin degeneracy, is

$$H_M = \sum_{i=0}^{2} \frac{\Delta_i}{2} \sigma_i^z + \sum_{i=1}^{2} \hbar \Omega \cos(\omega_0 t) \sigma_i^x, \tag{4}$$

where $i=0$ refers to the target spin and the spin operators are defined in the standard way $\boldsymbol{\sigma}_i = \Sigma_{\sigma\sigma'} c_{i\sigma}^{\dagger} \boldsymbol{\sigma}_{\sigma\sigma'} c_{i\sigma'}$ with $\boldsymbol{\sigma}$ being the vector of the 2×2 Pauli matrices. $\Delta_i = g_i \mu_B B_i$ is the Zeeman splitting due to a static magnetic field B_i along z, and a g factor g_i, Ω is the Rabi frequency, and ω_0 is the frequency of the oscillating magnetic field along x. For a single spin the oscillating magnetic field rotates the z component of the spin with frequency Ω when $\Delta = \hbar\omega_0$. We have ignored the effect of the oscillating field on the target spin which is a good approximation for narrow-band radiation that is only resonant with the spins on the DD (or alternatively only with the target spin), a condition that can be achieved, for example, by engineering different g factors in the dots and the target spin.

Moreover, we assume that the target spin interacts only with dot 1, although the basic idea can be extended to the most general case when the target spin interacts with both dots. As shown below our scheme is still efficient provided that the strength of the interaction between the target spin and each dot is different, a condition that is typically satisfied. We consider an Ising interaction between dot $i=1$ and the target spin $i=0$ of the form

$$H_I = \frac{J}{2} \sigma_0^z \sigma_1^z \tag{5}$$

with J being the strength of the interaction. J mainly depends on the distance of dot 1 from the target spin as well as the actual size of the dot and the target spin. Physical values for J for a purely dipolar interaction are within the range of a few megahertz as shown in Ref. 9. This form of interaction is justified when there is negligible tunnel coupling between dot 1 and the nearby spin so that to a good approximation hopping can be ignored. In addition, spin-flip processes are weak due to the Zeeman splitting induced by the static magnetic field and thus neglected. This is a good approximation when the difference in the Zeeman splittings between the target spin and the DD spins is much larger than the interaction strength J. Under these conditions the Ising interaction, Eq. (5), is a reasonable choice and leads to a nondemolition measurement.

The choice of Ising interaction dictates that the combination of DD system and target electron has to be specifically tailored to realize this nondemolition measurement. The necessary regime of parameters might be difficult to realize in a gate-defined quantum dot system, e.g., in GaAs but arises quite naturally in carbon nanotube dots probing a molecular spin. For example, with a typical dipole-dipole spin interaction strength of 5 MHz, a typical difference in Zeeman splitting of about 5% and a typical electron paramagnetic resonance Zeeman splitting of 10 MHz (see also Ref. 9) we arrive at a ratio of coupling strength to difference in Zeeman splitting of 10^{-2}. Considering the spin-flip terms as a perturbation to the diagonal Hamiltonian as in Ref. 11, the first-order corrections vanish and only second-order terms contribute, which are typically suppressed by a factor of 10^{-4}. This means that any spin-flip that can disturb the measurement will take place at a much reduced rate, thus making a

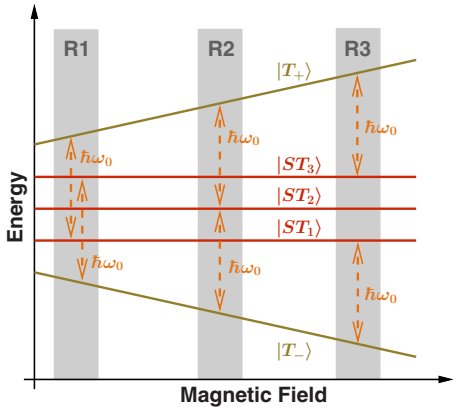

FIG. 2. (Color online) Schematic illustration of the two-electron energy diagram for the undriven system. ω_0 is the oscillating frequency of the driving field. $|T_+\rangle$ and $|T_+\rangle$ are blocked triplet states, $|ST_i\rangle, i=1,2,3$ are states with a singlet component. R1, R2, and R3 label regions of possible resonances.

nondemolition measurement possible (for details see Appendix).

For the DD with single orbital levels there are in total 16 states and the maximum number of electrons is 4. The many-body states of the DD and target spin system can be written in the form $|\mathrm{DD}\rangle|\sigma_T\rangle$, where $|\mathrm{DD}\rangle$ denotes the many-body states of the DD and $|\sigma_T\rangle=|\uparrow\rangle$ or $|\downarrow\rangle$ denotes the two possible target spin states. Starting with Eq. (2) we can define the two uncoupled spin up, H_S^{+1}, and spin down, H_S^{-1}, Hamiltonians in the subspace $|\mathrm{DD}\rangle|\uparrow\rangle$ and $|\mathrm{DD}\rangle|\downarrow\rangle$, respectively, depending on the state of the target spin. From Eqs. (3)–(5), it can be shown that

$$H_S^{\sigma} = H_{\mathrm{DD}} + \sigma\frac{\Delta_0}{2} + \frac{\Delta_1 + \sigma J}{2}\sigma_1^z + \frac{\Delta_2}{2}\sigma_2^z + \sum_{i=1}^{2}\hbar\Omega\,\cos(\omega_0 t)\sigma_i^x \tag{6}$$

with $\sigma=+1$ (-1) for target spin up (down).

Figure 2 shows schematically the two-electron energy-level diagram as function of the static magnetic field of the undriven system $(\Omega=0)$ and for spin up.[12] The upper and lower energy levels correspond to the triplets $|T_+\rangle$ and $|T_-\rangle$ which as explained in the next section lead to spin blockade. The remaining three energy levels, $|ST_i\rangle$, $i=1,2,3$ correspond to two-electron states that contain a singlet component and thus allow electronic transport. For the driven system $(\Omega\neq 0)$ transitions from the $|T_\pm\rangle$ to $|ST_i\rangle$ states can take place lifting the spin blockade and resulting in a change in the average occupation. Within a simplified approach if a transition frequency matches the frequency of the driving field the corresponding transition probability is expected to be high. The regions R1, R2, R3 in Fig. 2 illustrate such a resonant behavior. The magnetic field where the resonances occur depends on the energy splitting of the $|ST_i\rangle$ states and therefore on the interdot hopping γ and the coupling strength J. Additionally, as shown in the next section, interference effects, for instance, when $|T_\pm\rangle\rightarrow|ST_2\rangle$, can yield a vanishingly small probability for particular magnetic fields.

Having described the interaction of the DD with the oscillating magnetic field we analyze the dissipative interactions with the leads and the phonon heat bath. The left and right leads are described by a Hamiltonian of the form

$$H_{leads} = \sum_{\ell k\sigma}\epsilon_{\ell k}d_{\ell k\sigma}^{\dagger}d_{\ell k\sigma}, \tag{7}$$

where $d_{\ell k\sigma}^{\dagger}$ $(d_{\ell k\sigma})$ creates (annihilates) an electron in lead $\ell=\{L,R\}$ with momentum k, spin σ, and energy $\epsilon_{\ell k}$. The interaction between the dots and the leads is given by the tunneling Hamiltonian

$$H_T = \sum_{k\sigma}(t_L c_{1\sigma}^{\dagger}d_{Lk\sigma} + t_R c_{2\sigma}^{\dagger}d_{Rk\sigma}) + \mathrm{H.c.}, \tag{8}$$

where t_L (t_R) is the tunnel coupling between dot 1 (2) and lead L (R) and we consider the symmetric case with $t_L=t_R$.

To take into account spin relaxation we have considered a generic bosonic bath that is modeled as a set of harmonic oscillators and is described by the Hamiltonian

$$H_B = \sum_j \hbar\omega_{1,j}a_{1,j}^{\dagger}a_{1,j} + \sum_j \hbar\omega_{2,j}a_{2,j}^{\dagger}a_{2,j}. \tag{9}$$

We have assumed that each quantum dot is coupled to an independent bosonic bath and there are no environment-induced correlations between the two dots. The operators $a_{1,j}^{\dagger}$ $(a_{1,j})$ create (annihilate) a boson in mode j and similarly for $a_{2,j}^{\dagger}$ $(a_{2,j})$ while $\omega_{1,j}$ are the corresponding frequencies of the bath modes. The interaction between the bath and the spins of the DD is given by the general model Hamiltonian

$$H_{SB} = \sigma_1^{-}\sum_j \Lambda_{1,j}a_{1,j}^{\dagger} + \sigma_2^{-}\sum_j \Lambda_{2,j}a_{2,j}^{\dagger} + \mathrm{H.c.}, \tag{10}$$

where the spin-flip operators are $\sigma_i^{-}=c_{i\downarrow}^{\dagger}c_{i\uparrow}$ and $\Lambda_{1,j}$ $(\Lambda_{2,j})$ is the coupling constant between dot 1 (2) and the jth mode of the corresponding bath. H_{SB} allows spin-flip processes for electrons in the DD via energy exchange with the bath which, as shown in the next section, leads to a leakage current. We consider spin relaxation only in the DD since for the target spin an upper limit to its relaxation rate is set implicitly by the coupling to the leads. In our scheme the relaxation rate of the target spin has to be smaller than the electron tunneling rate from the leads to the DD to ensure a measurable change in the DD occupations before spin relaxation.

To investigate the electron occupation of the system we employ a master equation approach and derive an equation of motion for the reduced density matrix, ρ, for the system of interest that consists of the DD and the target spin.[13] The occupation probabilities are given by the diagonal elements of ρ. It is convenient to eliminate the time dependence from the system Hamiltonian H_S^{σ} and for this reason we perform a rotating-wave approximation.[13,14] This approximation is well justified for weak driving, i.e., when $\Omega\ll\omega_0$ as in our system. In the devices we are considering the ratio $\omega_0/\Omega_0 \gtrsim 1000$ but a recent experimental investigation shows that even for ratios $\omega_0/\Omega\approx 10$ the rotating-wave approximation still predicts the correct spin dynamics.[15] In the rotating frame an arbitrary system operator $\mathcal{K}$ is transformed as $U_z^{\dagger}\mathcal{K}U_z$ with the unitary operator $U_z=\exp(-i\sigma^z\omega_0 t/2)$ and $\sigma^z=\sum_{i=0}^{2}\sigma_i^z$.

Starting with the total density matrix, χ, and within the standard Born and Markov approximations[13] we derive an equation of motion for ρ by tracing over the leads and bosonic bath degrees of freedom, i.e., $\rho=\mathrm{Tr}_E\{\chi\}$, where $\mathrm{Tr}_E\{\cdots\}$ means trace over the environmental degrees of freedom. In the rotating frame and having performed a rotating-wave approximation the density matrix ρ satisfies the equation of motion,

$$\dot{\rho}(t) = \mathcal{L}_S\rho(t) + \mathcal{L}_{leads}\rho(t) + \mathcal{L}_B\rho(t) \tag{11}$$

with the free evolution term

$$\mathcal{L}_S\rho(t) = -\frac{i}{\hbar}[\mathcal{H}_S^\sigma, \rho(t)],$$

and the terms due to the electronic leads

$$\mathcal{L}_{leads}\rho(t) = -\frac{1}{\hbar^2}\mathrm{Tr}_E\left\{\int_0^\infty d\tau[H_T(t),[U(\tau)H_T(t-\tau)U^\dagger(\tau),\rho(t)\otimes\rho_{leads}]]\right\}$$

and the bosonic bath

$$\mathcal{L}_B\rho(t) = -\frac{1}{\hbar^2}\mathrm{Tr}_E\left\{\int_0^\infty d\tau[H_{SB}(t),[V(\tau)H_{SB}(t-\tau)V^\dagger(\tau),\rho(t)\otimes\rho_B]]\right\}.$$

The operators are $U(\tau)=\exp[-i(\mathcal{H}_S^\sigma+H_{leads})\tau/\hbar]$ and $V(\tau)=\exp[-i(\mathcal{H}_S^\sigma+H_B)\tau/\hbar]$ with ρ_{leads}, ρ_B being the equilibrium density matrix for the leads and the bosonic bath, respectively. The time-dependent operators are $c_{i\uparrow}(t)=c_{i\uparrow}\exp(-i\omega_0 t/2)$, $c_{i\downarrow}(t)=c_{i\downarrow}\exp(+i\omega_0 t/2)$ and the Hamiltonian $\mathcal{H}_S^\sigma$ depends on the nearby spin, $\sigma=+1$ (-1) for spin up (down), i.e.,

$$\mathcal{H}_S^\sigma = H_{\mathrm{DD}} + \sigma\frac{\delta_0}{2} + \frac{\delta_1+\sigma J}{2}\sigma_1^z + \frac{\delta_2}{2}\sigma_2^z + \sum_{i=1}^{2}\frac{\hbar\Omega}{2}\sigma_i^x \tag{12}$$

and we have introduced the magnetic field detuning $\delta_i=\Delta_i-\hbar\omega_0$.

For the numerical calculations we write Eq. (11) in the energy basis. This results in a system of 256 coupled equations for all the matrix elements of ρ which is solved numerically taking into account the normalization condition for the diagonal elements, $\Sigma_{i=1}^{16}\rho_{i,i}=1$. We are interested in the steady state, ρ_{st}, that corresponds to $\dot{\rho}=0$ in Eq. (11). The quantity of interest is the average electron occupation of the DD, for example, of dot 1, that is calculated as $N_1=\mathrm{Tr}\{n_1\rho_{st}\}$. In the next section we present the basic results and explain the influence of various system parameters on the average electron occupation of the DD.

III. INVESTIGATION OF SPIN METER

Before we examine the influence of microwave radiation we have to make a choice for the operating regime of the DD. DD systems and their physical response are highly tunable by adjusting the gate voltages and the source-drain bias voltage in the leads. A regime which is easily accessible and has attracted a lot of interest is the Pauli spin blockade regime which has been demonstrated experimentally in various systems such as AlGaAs/GaAs and Si/Ge double quantum dots[16,17] as well as carbon nanotube dots.[18] In this regime one electron is confined in each dot and the three triplet states are almost equally and fully populated. In the absence of spin relaxation and microwaves the (1,1) triplet states are blocked from moving on to a (0,2) state by the Pauli exclusion principle [(n,m) denotes a charge state with n (m) electrons on dot 1 (2)]. Thus the electrical current as a function of the source-drain bias is suppressed.

For a fixed source-drain bias in the spin blockade regime a change in the occupations of the two dots can occur and a microwave-induced current can flow provided that the two dots have a different Zeeman splitting.[19] In this case the oscillating magnetic field in combination with a static field induces coherent spin rotations that mix two-electron states and current flows through the transport cycle $(0,1)\rightarrow(1,1)\rightarrow(0,2)\rightarrow(0,1)$. When the two dots have the same Zeeman splitting the spins in the two dots rotate at the same rate in the triplet subspace and therefore the average occupation remains fixed and current does not flow.[19,20] In this case only spin relaxation can give rise to a change in the occupation of the dots.

Inspection of the σ_i^z terms in Hamiltonian (12) shows that the interaction of the nearby spin with the spins on dot 1 induces an effective Zeeman asymmetry between the two dots of order J that depends on the orientation of the nearby spin. This suggests that a microwave-induced change in the occupation of the DD could take place and reveal information about the spin state when the dot parameters are adjusted to the spin blockade regime.

A Zeeman asymmetry can, in principle, arise due to intrinsic factors as in the case whereby the two coupled dots have different g factors leading to $\Delta_1\neq\Delta_2$, which could make the spin detection difficult. In Ref. 21 we have shown how to detect a magnetic field gradient and/or a difference in the g factors in the absence of the nearby spin that corresponds to $J=0$. Within our scheme spin detection is efficient when the intrinsic Zeeman asymmetry is much smaller than the spin interaction, i.e., when $|\Delta_1-\Delta_2|\ll J$. Nevertheless, in

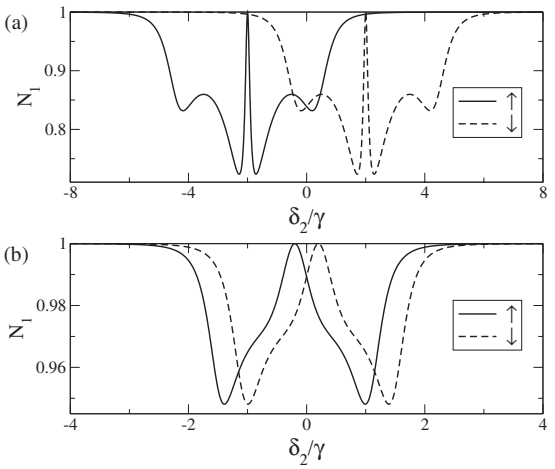

FIG. 3. (a) Average occupation of dot 1 as a function of the magnetic field detuning δ_2 when the target spin is up (solid line) and down (dashed line), for the parameters $J=4\gamma$, $\gamma=1.5\times10^{-6}U$, $k_BT=U/100$, $\hbar\Omega=10^{-6}U$, and $\hbar\omega_0=10^{-3}U$. (b) The same as in (a) for $J=0.4\gamma$.

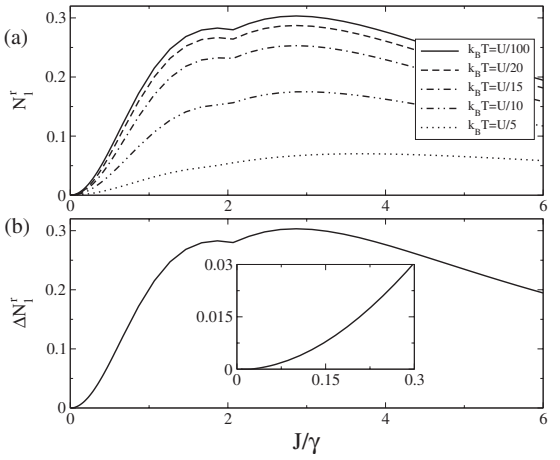

FIG. 4. (a) Microwave-induced change in the occupation of dot 1 as a function of the interaction strength J for different temperatures and when the target spin is up and $\gamma=1.5\times10^{-6}U$, $\hbar\Omega=10^{-6}U$, and $\hbar\omega_0=10^{-3}U$. (b) Maximum difference of the spin up and spin down occupations for the same parameters as in (a) with $k_BT=U/100$. The inset is an enlarged view for small J.

this work we assume for simplicity that $\Delta_1=\Delta_2$ and thus the Zeeman asymmetry is due entirely to the presence of the nearby spin, and further that J is independent of the applied magnetic field.

For the numerical calculations the internal parameters of the DD are adjusted to zero-energy detuning and specifically we choose $E(1,1)-E(0,2)=0$, with $E(n,m)$ being the energy of the charge state (n,m). For a practical realization this configuration could be achieved via adjusting the gate voltages that define the confining potential of the DD.[20] We choose for the on-site energies $\varepsilon_1=-U/2$, $\varepsilon_2=-U$ and for the interdot Coulomb energy $V=U/2$.[22] The bias voltage is $V_{sd}=(\mu_L-\mu_R)/e=U/2e$ and it is applied symmetrically, thus $\mu_L=U/4$ and $\mu_R=-U/4$, with μ_L (μ_R) being the chemical potential of the left (right) lead. When the interdot hopping satisfies $\gamma\ll U$ and the temperature $k_BT\lesssim U/80$ the current as a function of source-drain bias is suppressed due to spin blockade and each dot contains a single electron.

Figure 3(a) shows the average electron occupation of dot 1 as a function of the magnetic field detuning δ_2 for the two possible states of the target spin. We consider no spin relaxation and therefore we set $\Lambda_{1,j}=\Lambda_{2,j}=0$ in Eq. (10). The dot occupation exhibits resonances (peaks) due to intradot spin rotations induced by the oscillating magnetic field and interdot tunneling, and it is constant close to unity far from the resonances due to spin blockade. For each spin configuration there are in total four peaks whose positions depend on γ and J. The two outer peaks correspond to resonances R1 and R3 (see Fig. 2) and we would expect a third resonance at $\hbar\omega_0=(\Delta_1+\Delta_2\pm J)/2$, corresponding to R2, but this resonance is split by an antiresonance, resulting in the two inner peaks. In terms of spin-dependent detuning the condition for the antiresonance is $|\delta_1\pm J|=|\delta_2|$. This very symmetric situation together with the microwave driving leads to the emergence of an eigenstate of the system with purely (1,1) triplet components, resulting in spin blockade. It can be shown from the steady-state occupations that for this detuning the $|S_{02}\rangle=|0,\uparrow\downarrow\rangle$ state is unoccupied and the current is suppressed.

Away from the symmetry point, when $\kappa>\gamma\hbar\Omega/J$, defining the distance from the symmetry point as $\kappa=|\delta_1\pm J|-|\delta_2|$, the eigenstate is no longer a pure triplet and current can flow, resulting in the two inner peaks left and right of the antiresonance. We can try to gain an intuitive understanding of the outer peak positions. Naively one would expect the outer peaks to appear when either the spin in dot 1 is on resonance or the spin in dot 2 is on resonance. However, for finite interdot hopping the outer peaks are somewhat shifted from the positions that one would expect for independent spins since intradot spin rotations take place with interdot hopping. As a result the shift is large when γ is large. Interdot hopping leads to delocalization of the electron spins via the resonant coherent transitions $|\uparrow,\downarrow\rangle\leftrightarrow|0,\uparrow\downarrow\rangle$ and $|\downarrow,\uparrow\rangle\leftrightarrow|0,\uparrow\downarrow\rangle$, with an amplitude proportional to γ, that populate the $|0,\uparrow\downarrow\rangle$ state and thus lead to a change in the populations. In addition, the populations of the $|\uparrow,\downarrow\rangle$ and $|\downarrow,\uparrow\rangle$ states are unequal leading to a mixing of the (1,1) singlet and the $S_z=0$ triplet that depends on the magnitude of J and γ. When J is small the two outer peaks overlap with the inner peaks as shown, for example, in Fig. 3(b), though the important point is that the spin up and spin down signals can still be distinguished (see also below) making the measurement feasible. When $J=0$ resonances do not occur since the spins in the two dots rotate at the same rate and the $|S_{02}\rangle$ state remains unoccupied.

The change in the dot occupation is large when the Rabi frequency, Ω, is smaller than $\gamma/\hbar$ or the same order of magnitude, a condition that allows interdot hopping while intradot spin rotations take place. In the opposite limit spin rotations dominate and the average dot occupation remains close to unity in both dots. If J is much smaller than γ the mixing of two-electron states is weak, whereas in the opposite limit interdot transitions are suppressed and the microwaves have no significant effect resulting in a rather small resonant change. Therefore, probing a small J needs a small γ.

To quantify this effect we show in Fig. 4(a) the relative occupation on resonance as a function of J, for a fixed inter-

dot hopping and for different temperatures, when the nearby spin is up. A spin down results in the same behavior. The relative occupation of dot 1, N_1^r, is calculated as $N_1^r = N_1^0 - N_1^p$, where N_1^p is the occupation on resonance, i.e., the value of the occupation at the strongest peak, and N_1^0 is the occupation off resonance (background occupation). The weak feature in the curves at $J \approx 2\gamma$ is due to the outer peaks (R1 and R3 regions in Fig. 2) becoming distinguishable from the inner peaks (R2 region). For temperatures $k_B T \lesssim U/80$, the background occupation is fixed $N_1^0 \approx 1$, due to spin blockade and hence the relative occupation is essentially temperature independent. In this regime there is to good approximation one electron in each dot in the $|T_\pm\rangle$ states. With increasing temperature spin blockade is gradually lifted and the background occupation increases. All one- and two-electron states acquire a finite population and even three-electron states, for instance, (1,2), become occupied and have to be included in the dynamics of the density matrix. This happens since the lengthening tail of the Fermi-Dirac distribution of the lead electrons leads to the opening of additional transport channels. The exact temperature dependence of N_1^r depends on various factors such as coupling to the leads, spin relaxation rate, as well as the applied source-drain bias. Even though this dependence may not be monotonic in all cases for high enough temperatures ($k_B T \gtrsim U$) the resonances cannot be clearly resolved and $N_1^r \approx 0$. From Fig. 4(a) we conclude that the DD detector has a higher temperature range of operation compared with a single dot since the charging energy is the relevant energy scale. A similar increase in operating temperature has been predicted for an undriven DD read-out of a charge qubit.[23]

In a spin read-out situation we are not only interested in the height of the resonant peaks but we want to distinguish two target spin states. Thus, the figure of merit for a spin read-out has to be the maximum difference in population for target spin up and target spin down. In Fig. 4(b) we plot the maximum difference ΔN_1^r of the spin up and spin down occupations as a function of J and for a fixed interdot hopping. For $J \gtrsim 2\gamma$ the maximum difference occurs at the inner peak of the spin up (down) occupation with $\delta_2 < 0$ ($\delta_2 > 0$). The results indicate that a large difference can be induced making possible the discrimination between spin up and spin down states.

As shown above, the achievable difference in dot occupation depends on a range of parameters. Figure 5 shows a contour plot of the average occupation as a function of detuning and interdot hopping for a fixed spin interaction strength.[24] The occupation exhibits a distinct resonant pattern for both spin up and down and further it enables the two possible outcomes to be distinguished in a range of interdot hopping. Our calculations confirm that this is a robust behavior that occurs for other values of J in the range $\sim(10^{-7}-10^{-6})U$. However, as explained above for $\gamma \gg J$ the occupation peaks decrease and this could make the spin detection relatively difficult.

In addition to the temperature effect the background average occupation increases due to spin relaxation and as a result the microwave-induced resonances cannot be clearly resolved since the relative occupation in both dots drops. Spin relaxation and decoherence will also influence the peak

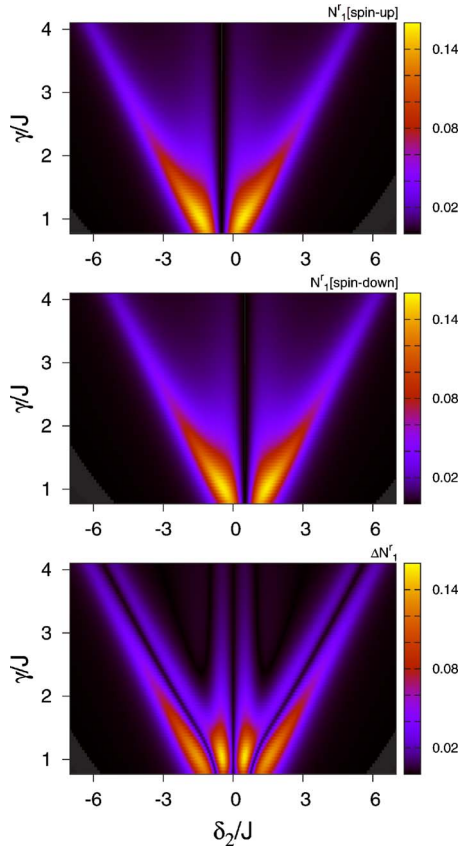

FIG. 5. (Color online) Relative occupation of dot 1 as a function of magnetic field detuning δ_2 and interdot hopping γ for spin up and down for the parameters $J = 9 \times 10^{-7} U$, $k_B T = U/100$, $\hbar\Omega = 10^{-6} U$, and $\hbar\omega_0 = 10^{-3} U$. The lower frame shows the absolute difference of the spin up and spin down occupations.

height of the resonances since they inhibit coherent spin rotations. Spin-flip processes which take place because of the interaction of the DD spins with the bosonic bath described by Eq. (10), allow incoherent transitions between two-electron states, for example, $|\uparrow,\uparrow\rangle \leftrightarrow |\downarrow,\uparrow\rangle$, $|\uparrow,\downarrow\rangle$, which in turn populate the $|S_{02}\rangle$ state, lifting the spin blockade, and thus increasing the background occupation. This happens even in the absence of the nearby spin, i.e., when $J=0$, though spin blockade can still be recovered as shown in Ref. 19 depending on the spin relaxation rate and the coupling to the leads.

To examine the effect of spin relaxation on the driven DD spin detector we have calculated the change in population for various spin relaxation rates γ_s. Results are shown in Fig. 6 for the relative occupation of the strongest (outer) peaks as a function of hopping when the nearby spin is up (the same behavior results for spin down). We have taken $\gamma_s = \pi|\Lambda|^2 D(\delta\epsilon)[2n(\delta\epsilon, T) - 1]/\hbar$ with the Bose function $n(\delta\epsilon, T) = [\exp(\delta\epsilon/k_B T) - 1]^{-1}$ and $\delta\epsilon = \hbar\omega_0$. D is the density of states for the bosonic bath that is taken constant and also $|\Lambda| = |\Lambda_{1,j}| = |\Lambda_{2,j}|$ in Eq. (10). This expression for γ_s can be derived by assuming a single spin with Zeeman splitting $\delta\varepsilon$ coupled to a bosonic bath at temperature T which we assume to be the same as the temperature in the leads. We focus on the most interesting experimental regime in which the spin

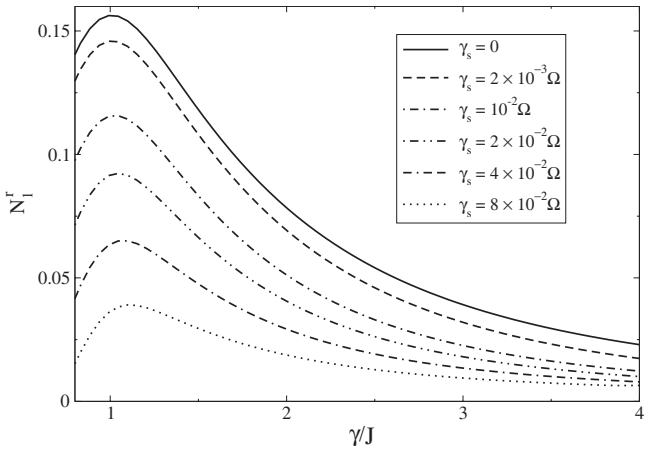

FIG. 6. Relative occupation of dot 1 as a function of the interdot hopping for different spin relaxation rates when the target spin is up and the parameters $J=9\times10^{-7}U$, $k_BT=U/100$, $\hbar\Omega=10^{-6}U$, and $\hbar\omega_0=10^{-3}U$. A spin down shows the same behavior.

relaxation rate is much smaller than the tunneling rate through the DD and the system weakly deviates from the spin blockade regime. As seen in Fig. 6, the effect of spin relaxation becomes important as γ_s increases, which in turn leads to a decrease in the relative occupation. The sensitivity of the spin detector is limited by the minimum detectable change in the occupations. The optimum resolution can be achieved when the driving is efficient. This happens when the Rabi frequency, which is controlled by the intensity of the oscillating field, is larger than the spin relaxation rate of the dot spins and the target spin, as well as the tunneling rate through the DD.

IV. DISCUSSION AND CONCLUSIONS

In summary, we have suggested an electrical scheme to probe a single spin which makes use of two serially tunnel-coupled quantum dots connected to metallic leads. The spin is located at some distance from the dots, which has to be smaller than the typical interdot separation, and the total system is in a static magnetic field under the application of a microwave magnetic field. The spin interacts with the spins on the dots and this interaction results in an effective Zeeman splitting that is different in the two dots. Due to an electron-spin-resonance effect the electron occupations of the dots exhibit resonances which reveal information about the state of the nearby spin. In particular, the ac-driven DD spin meter provides an explicit signal in the induced occupations for both spin orientations and enables the spin state to be probed noninvasively in a single shot provided that the target spin has a different g factor from the DD system, a condition that is typically satisfied.

In order to detect the resonant change in occupation, a charge detector, e.g., a quantum point contact (QPC) or a single-electron transistor (SET) has to be employed. As long as the bias voltage of the QPC/SET is smaller than the level spacing on the DD, it will not influence the operation of the device as a spin meter. A further source of error would be an inaccurate charge detector, whereby the recorded electron count does not correspond to the actual electron count. However, provided the miscount is smaller than the average change in population, spin up and spin down can still be distinguished.

We identified a range of parameters for which the DD spin meter can operate and analyzed how we can tune its sensitivity with the interdot hopping and intensity of the microwave field that defines the Rabi frequency for spin rotations. The operation of the DD spin meter depends on a lifting of a Pauli spin blockade, and therefore it can operate at much higher temperatures than the single dot which is limited to temperatures comparable to the Zeeman energy.[9] For instance, for a charging energy of 10 meV and spin-spin interaction strength in the range ~5 MHz the resonances survive up to temperatures of a few tens of kelvins. To achieve a similar operating temperature with a single dot, magnetic fields of a few tens of teslas and correspondingly microwave frequencies of several hundreds of gigahertz would be necessary, conditions which are available only in specialized laboratories. The sensitivity of the meter is limited by internal spin relaxation which essentially leads to a small change in the occupations and as a consequence the resonances cannot be clearly resolved. For an efficient read-out the tunneling rates from dots to leads and the microwave-induced Rabi frequency have to be larger than all the relevant spin relaxation rates.

Finally, the change in population effected by the microwave field has to be seen in relation to the relaxation time of the target spin. On one hand, the spin read-out has to be completed within the relaxation time of the target spin, otherwise random spin-flips will obscure the result. On the other hand, for a given change in population, ΔN_i, of dot $i=1,2$ a certain number of electrons, n, has to pass through the DD and be counted by the charge detector. To achieve reliable statistics the requirement $n>1/\Delta N_i^2$ has to be fulfilled since then fluctuations in the average number are smaller than the change in population that we want to distinguish. At a given tunneling rate Γ through the device, this determines the minimum time of the measurement $T_m=n/\Gamma=1/(\Gamma\Delta N_i^2)<T_1$, which must be smaller than the spin relaxation time of the target spin. We arrive therefore at a minimum tunneling rate through the dot, $\Gamma>1/(\Delta N_i^2 T_1)$. However, we are not free to increase the tunneling rate arbitrarily; once the tunneling rate approaches the Rabi frequency the resonance peaks in the population are suppressed. By demanding $10\Gamma<\Omega$ we obtain the minimum resolvable change in population as $\Delta N_i=\sqrt{10/(T_1\Omega)}$.

We conclude by estimating the feasibility of measuring the state of a molecular spin system, for example, $Sc@C_{82}$, which can be coupled with a carbon nanotube DD.[18] Such carbon-based systems are promising candidates for quantum information processing and around several kelvins have a $T_1\approx1$ s (Refs. 25 and 26). Then with a Rabi frequency of 10 MHz we arrive at a minimum resolvable change in population of $\Delta N_i=0.001$. An interdot hopping of $\gamma=10$ MHz and a spin-spin interaction of $J\approx5$ MHz (see Ref. 9 for an estimation of J) would lead to $\Delta N_i\approx0.07$ in the case of no spin decoherence. With a spin decoherence rate of $\gamma_s=1$ MHz this reduces to $\Delta N_i\approx0.007$. In order to be able to resolve such a difference in occupation, spin-flip processes have to

be sufficiently suppressed by a difference in Zeeman splitting of the target and the dot spin (see Appendix). To resolve $\Delta N_i \approx 0.007$ with $\Omega = 10$ MHz a difference in Zeeman splitting $\delta\Delta \approx 1$ GHz is needed. For a g factor of $g=2$ for the molecule and $g=2.1$ for the carbon nanotube[27] this results in a required microwave frequency of $\omega_0 \approx 20$ GHz. Considering all estimates a single spin read-out with realistic parameters at liquid-helium temperatures is feasible.

ACKNOWLEDGMENTS

We would like to thank Mark Buitelaar for discussions. The work is part of the UK QIP IRC (Grant No. GR/S82176/01). J.W. thanks the Wenner-Gren Foundations for financial support. B.W.L. thanks the Royal Society. J.H.J. acknowledges support from the UK MoD. G.A.D.B. is supported by EPSRC (Grant No. GR/S15808/01).

APPENDIX: DERIVATION OF EFFECTIVE ISING COUPLING

Consider two spins with different Zeeman splittings described by the Hamiltonian

$$H_0 = \frac{\Delta}{2}\sigma_A^z + \frac{\Delta+\delta\Delta}{2}\sigma_B^z, \tag{A1}$$

where Δ ($\Delta+\delta\Delta$) denotes the Zeeman splitting of spin A (B) and $\delta\Delta$ the difference in Zeeman splitting between spin A and spin B. In this analysis spin B is the target spin, which interacts with spin A via an isotropic Heisenberg interaction given by

$$H_1 = \frac{J}{2}(\sigma_A^x\sigma_B^x + \sigma_A^y\sigma_B^y + \sigma_A^z\sigma_B^z), \tag{A2}$$

where J denotes the strength of the interaction. In addition to the diagonal contribution $\sigma_A^z\sigma_B^z$, the Heisenberg Hamiltonian couples spin states which differ in energy by $\delta\Delta$ via $\sigma_A^x\sigma_B^x + \sigma_A^y\sigma_B^y$, and we can treat the Hamiltonian H_1 as a perturbation to the Hamiltonian H_0. The eigenstates of the unperturbed Hamiltonian are the spin states $|\psi_1^{(0)}\rangle = |\uparrow\uparrow\rangle$, $|\psi_2^{(0)}\rangle = |\uparrow\downarrow\rangle$, $|\psi_3^{(0)}\rangle = |\downarrow\uparrow\rangle$, and $|\psi_4^{(0)}\rangle = |\downarrow\downarrow\rangle$ and so the first-order correction to the energy eigenvalues becomes

$$E_i^{(1)} = \langle\psi_i^{(0)}|H_1|\psi_i^{(0)}\rangle. \tag{A3}$$

We can therefore write the Hamiltonian including the first-order correction as

$$H = \frac{\Delta}{2}\sigma_A^z + \frac{\Delta+\delta\Delta}{2}\sigma_B^z + \frac{J}{2}\sigma_A^z\sigma_B^z. \tag{A4}$$

The free Hamiltonian of spin B commutes with H. The new eigenstates are found using the standard formula

$$|\psi_i\rangle = |\psi_i^{(0)}\rangle + \sum_{i\neq j}\frac{\langle\psi_i^{(0)}|H_1|\psi_j^{(0)}\rangle}{E_i^{(0)} - E_j^{(0)}}|\psi_j^{(0)}\rangle, \tag{A5}$$

which gives $|\psi_1\rangle = |\uparrow\uparrow\rangle$, $|\psi_2\rangle = |\uparrow\downarrow\rangle - J/\delta\Delta|\downarrow\uparrow\rangle$, $|\psi_3\rangle = |\downarrow\uparrow\rangle + J/\delta\Delta|\uparrow\downarrow\rangle$, and $|\psi_4\rangle = |\downarrow\downarrow\rangle$. Typically the difference in Zeeman splitting $\delta\Delta$ is at least two orders of magnitude larger than the Heisenberg interaction strength J, resulting in a very small admixture of $|\downarrow\uparrow\rangle$ ($|\uparrow\downarrow\rangle$) in the eigenstate $|\psi_2\rangle$ ($|\psi_3\rangle$). This leads to a very small but finite probability for a spin-flip in spin B.

Consider now the situation in which a current is flowing through the DD adjacent to the target spin. If a target spin-flip can take place a channel for decoherence exists via the coupling to the lead electrons. The decoherence rate has to be proportional to the tunneling rate through the device, Γ, and is suppressed by the reduced probability for a spin-flip, resulting in the effective decoherence rate for the target spin given by $\Gamma(J/\delta\Delta)^2$, and a corresponding coherence time $T_{cJ} = 1/\Gamma(J/\delta\Delta)^2$. The measurement has to be done within this coherence time and the information about the initial target spin state is scrambled. If we compare this coherence time with the measurement time $T_m = 1/\Gamma\Delta N_i^2$, we conclude that the minimum resolvable change in occupation number is given by $\Delta N_{iJ} = J/\delta\Delta$. The off-resonant microwave radiation can be treated similarly, resulting in a coherence time $T_{c\Omega} = 1/\Gamma(\hbar\Omega/\delta\Delta)^2$. The minimum resolvable number difference is then $\max(\Delta N_{iJ}, \Delta N_{i\Omega})$.

[1] F. H. L. Koppens, C. Buizert, K. J. Tielrooij, I. T. Vink, K. C. Nowack, T. Meunier, L. P. Kouwenhoven, and L. M. K. Vandersypen, Nature (London) **442**, 766 (2006).
[2] J. R. Petta, A. C. Johnson, J. M. Taylor, E. A. Laird, A. Yacoby, M. D. Lukin, C. M. Marcus, M. P. Hanson, and A. C. Gossard, Science **309**, 2180 (2005).
[3] J. M. Elzerman, R. Hanson, L. H. Willems van Beveren, B. Witkamp, L. M. K. Vandersypen, and L. P. Kouwenhoven, Nature (London) **430**, 431 (2004).
[4] D. Rugar, R. Budakian, H. J. Mamin, and B. W. Chui, Nature (London) **430**, 329 (2004).
[5] E. Cota, R. Aguado, and G. Platero, Phys. Rev. Lett. **94**, 107202 (2005).
[6] R. Sánchez, E. Cota, R. Aguado, and G. Platero, Phys. Rev. B **74**, 035326 (2006).
[7] S. D. Barrett and T. M. Stace, Phys. Rev. Lett. **96**, 017405 (2006).
[8] H.-A. Engel, V. N. Golovach, D. Loss, L. M. K. Vandersypen, J. M. Elzerman, R. Hanson, and L. P. Kouwenhoven, Phys. Rev. Lett. **93**, 106804 (2004).
[9] J. Wabnig and B. W. Lovett, New J. Phys. **11**, 043031 (2009).
[10] A single orbital description is also valid for carbon nanotube quantum dots when the valley degeneracy is broken and the induced single-particle splitting is large. See, for example, Ref. 18.
[11] J. A. Weil and J. R. Bolton, *Electron Paramagnetic Resonance: Elementary Theory and Practical Applications* (Wiley, New York, 2007).
[12] We are interested in static magnetic fields which produce a Zeeman splitting on the order of $\hbar\omega_0$, and small interdot hoppings

and spin interaction strengths. In this regime the $|T_-\rangle$ ($|T_+\rangle$) is the lowest (highest) two-electron state.

[13] C. W. Gardiner and P. Zoller, *Quantum Noise* (Springer, New York, 2000).

[14] J. Wabnig, B. W. Lovett, J. H. Jefferson, and G. A. D. Briggs, Phys. Rev. Lett. **102**, 016802 (2009).

[15] G. D. Fuchs, V. V. Dobrovitski, D. M. Toyli, F. J. Heremans, and D. D. Awschalom, Science **326**, 1520 (2009).

[16] K. Ono, D. G. Austing, Y. Tokura, and S. Tarucha, Science **297**, 1313 (2002).

[17] N. Shaji, C. B. Simmons, M. Thalakulam, L. J. Klein, H. Qin, H. Luo, D. E. Savage, M. G. Lagally, A. J. Rimberg, R. Joynt, M. Friesen, R. H. Blick, S. N. Coppersmith, and M. A. Eriksson, Nat. Phys. **4**, 540 (2008).

[18] M. R. Buitelaar, J. Fransson, A. L. Cantone, C. G. Smith, D. Anderson, G. A. C. Jones, A. Ardavan, A. N. Khlobystov, A. A. R. Watt, K. Porfyrakis, and G. A. D. Briggs, Phys. Rev. B **77**, 245439 (2008).

[19] R. Sánchez, C. López-Monís, and G. Platero, Phys. Rev. B **77**, 165312 (2008).

[20] F. H. L. Koppens, C. Buizert, I. T. Vink, K. C. Nowack, T. Meunier, L. P. Kouwenhoven, and L. M. K. Vandersypen, J. Appl. Phys. **101**, 081706 (2007).

[21] G. Giavaras, J. Wabnig, B. W. Lovett, J. H. Jefferson, and G. A. D. Briggs, Physica E (Amsterdam) **42**, 895 (2010).

[22] The exact value of V does not affect the main conclusions as long as $\gamma \ll U$ and the DD parameters are adjusted to zero-energy detuning.

[23] T. Gilad and S. A. Gurvitz, Phys. Rev. Lett. **97**, 116806 (2006).

[24] The interdot hopping cannot be made arbitrarily small since this will invalidate the Born approximation.

[25] A. Ardavan, M. Austwick, S. C. Benjamin, G. A. D. Briggs, T. J. S. Dennis, A. Ferguson, D. G. Hasko, M. Kanai, A. N. Khlobystov, B. W. Lovett, G. W. Morley, R. A. Oliver, D. G. Pettifor, K. Porfyrakis, J. H. Reina, J. H. Rice, J. D. Smith, R. A. Taylor, D. A. Williams, C. Adelmann, H. Mariette, and R. J. Hamers, Philos. Trans. R. Soc. London, Ser. A **361**, 1473 (2003).

[26] S. C. Benjamin, A. Ardavan, G. A. D. Briggs, D. A. Britz, D. Gunlycke, J. Jefferson, M. A. G. Jones, D. F. Leigh, B. W. Lovett, A. N. Khlobystov, S. A. Lyon, J. J. L. Morton, K. Porfyrakis, M. R. Sambrook, and A. M. Tyryshkin, J. Phys.: Condens. Matter **18**, S867 (2006).

[27] F. Kuemmeth, S. Ilani, D. C. Ralph, and P. L. McEuen, Nature (London) **452**, 448 (2008).